

Short Research Article

Structural design and hydrodynamic coefficient calculation of observation-class ROVs

Abstract

Tethered Underwater Robot (Remote Operated Vehicle, ROV) Tethered underwater robots (ROVs) can replace humans in inspecting and maintaining water facilities such as reservoirs and dams. Connected to surface support equipment through umbilical cables, the umbilical cable allows the operator to control the ROV's operations remotely from a mother ship or shore. Using the ROV as an underwater operational platform, precise and efficient underwater inspection and repair operations for hydraulic structures can be achieved by mounting underwater mechanical arms, pan-tilt cameras, cleaning and cutting devices, etc. This paper designs an observation-class ROV, carries out structural design of the ROV body, selects and models sensors and actuators according to actual needs, and provides a method for using the FLUENT software to perform hydrodynamic calculations and obtain hydrodynamic coefficients based on the model.

Keywords:ROV, hydrodynamic calculation, FLUENT

1 Introduction

With the development of underwater robot technology, underwater robots are gradually replacing human underwater operations due to their high work efficiency, ease of operation, safety, and reliability. The foreign application of ROVs began in the 1950s, with "CURV1" being the first ROV produced in the world, born in the United States in 1960. Japan also has significant technical advantages in the field of ROVs. The Japan Marine Science and Technology Center successfully developed the "Dolphin 3K" in 1987^[1], and only a year later, successfully developed the "Trench" ^[2]10,000-meter class ROV. China's first ROV, "Hairen No.1", was jointly developed by the Shenyang Institute of Automation of the Chinese Academy of Sciences and Shanghai Jiaotong University in ^[3]the late 1970s. Over the following decades, substantial progress was made, with many large, medium, and small ROVs being developed, such as the "Sea Dragon" ^[4]and "Seahorse"^[5].

The hydrodynamic coefficient is an important parameter in the dynamics equation of underwater robots, which can characterize the underwater motion characteristics of underwater robots with different structures. At present, the methods to solve the hydrodynamic coefficient mainly include empirical formula estimation, ship model test, and Computational Fluid Dynamics (CFD) numerical simulation. The accuracy of the empirical formula estimation method is relatively lower than the latter two and is mostly used for inertial hydrodynamic coefficient calculations and hydrodynamic coefficient calculations that do not significantly affect the model calculation results of the second order and above. The accuracy of the hydrodynamic coefficient obtained by the ship model test method is the highest among these three methods, but the cost and requirements of the test equipment are high. The method of simulating ship model tests using CFD technology has advantages such as being unaffected by the accuracy of the test equipment and low cost, and can provide an ideal simulation environment that is not disturbed by the external environment, so it is widely used to calculate the hydrodynamic coefficients of underwater vehicles^[6].

This paper designs an observation-class ROV for inspecting and maintaining water facilities such as reservoirs and dams, and uses the FLUENT software to solve its hydrodynamic coefficient.

1 ROV Structural Design and Equipment Selection

The main parts of the ROV body include: external frame, electronic sealing cabin, thruster, camera, lighting equipment, mechanical arm, and buoyancy part^[7]. The external frame mainly plays a supporting role and can also protect the equipment located inside the frame. Most equipment is also directly fixed on the external frame of the ROV.

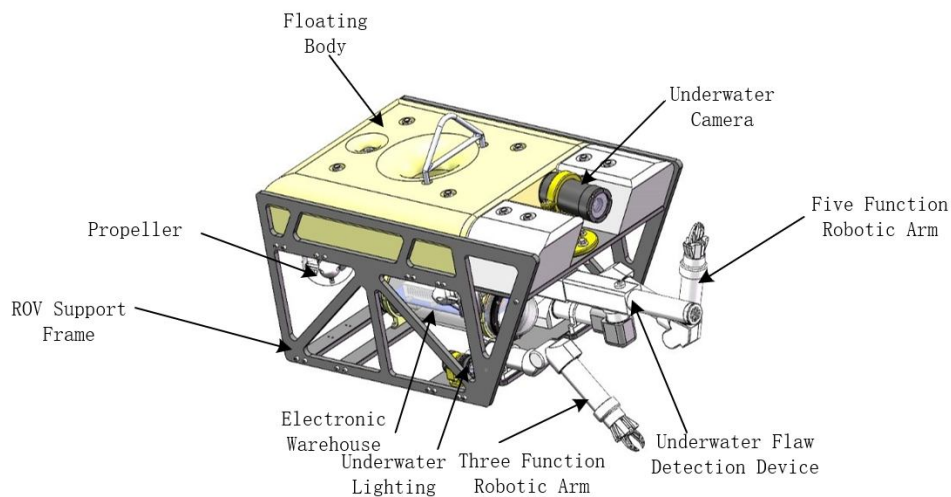
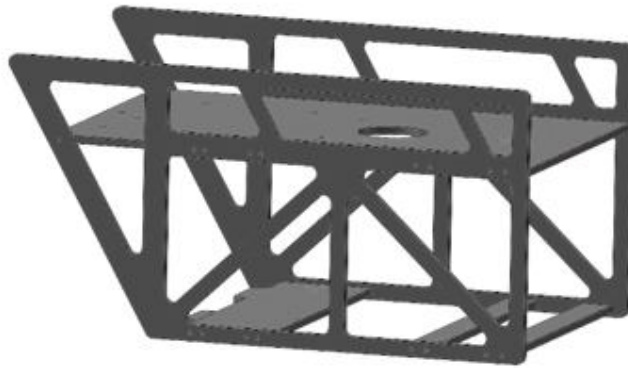


Figure 1 Overall schematic diagram of ROV

1.1 External Frame Design

ABS plastic has the advantages of high strength, strong impact resistance, and scratch resistance. The strong corrosion resistance is the biggest highlight of ABS plastic, which can meet the demand for long-term underwater applications. The lower part of the external frame is composed of multiple support plates, which are fixed with two side plates using bolts. The lower support plate also serves as a fixed bracket for equipment such as electronic warehouses, lighting equipment, depth gauges, mechanical arms, etc. The upper support plate is a whole piece of ABS plastic plate, and the buoy, underwater camera, and thruster are fixed on the upper support plate, also using several pairs of bolts to connect with the two side



plates.

Figure 2 ROV External framework

1.2 Design of Electronic Sealing Cabin

The electronic sealing cabin, as a waterproof device for the power supply equipment and control equipment of the underwater robot, needs to ensure that all electrical equipment in the sealed cabin is separated from the underwater environment. The sealing cabin interface must be tightly sealed and needs to have enough pressure resistance^[8]. Various electrical equipment installed inside the sealed cabin need to work together, and to make the limited space more efficiently used, a partition is added in the middle of the sealed cabin to divide the internal space into two semicylindrical shapes, and the electrical equipment can be arranged in order.

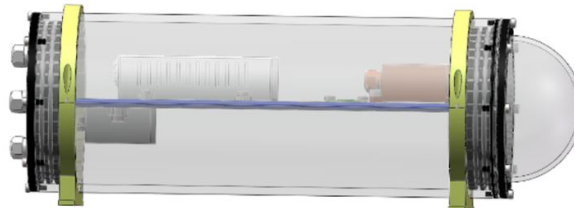


Figure 3 Electronic warehouse

1.3 Thruster

The ROVMAKER T200 electric thruster is selected as the thruster. This model is widely used in observation-class ROVs and aquatic equipment. It is made of underwater corrosion-resistant materials and only weighs 156g in water. Under such a light premise, the maximum thrust can reach 5kg. Because it has a light weight and good performance, this model of thruster is more suitable for observation-class underwater robots and more in line

with the actual needs of the design. Choosing this model of thruster can meet the design requirements.

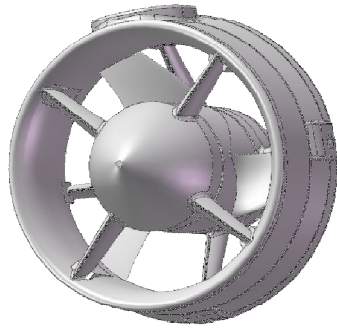


Figure 4 Propeller



Figure 5 Underwater lighting

1.4 Underwater Lighting

The underwater lighting system uses the ROVMAKER underwater light, which is a light specifically for underwater use. It has the characteristics of high brightness, deep pressure resistance, and long life. Made of aluminum alloy material, it has high underwater heat dissipation efficiency, small size, and light weight. The use depth can reach 500 meters, meeting the design requirements, and can be applied in environments such as reservoirs, dams, lakes for inspection and operation equipment.

1.5 Underwater Camera Device

The underwater camera system uses the ZF-IPC-02B11-ALPLPFS model underwater camera from ZF Tech. It supports 1080p HD video, has built-in image enhancement functions, and can defog underwater, providing good imaging results even in murky water. The casing is made of stainless steel/aluminum alloy material, which can resist water and rust for a long time and can operate normally under 500 meters of water pressure. At the same time, it is compatible with most video communication protocols on the market such as TCP/IP, UDP, RTP, RTSP, demonstrating good compatibility.

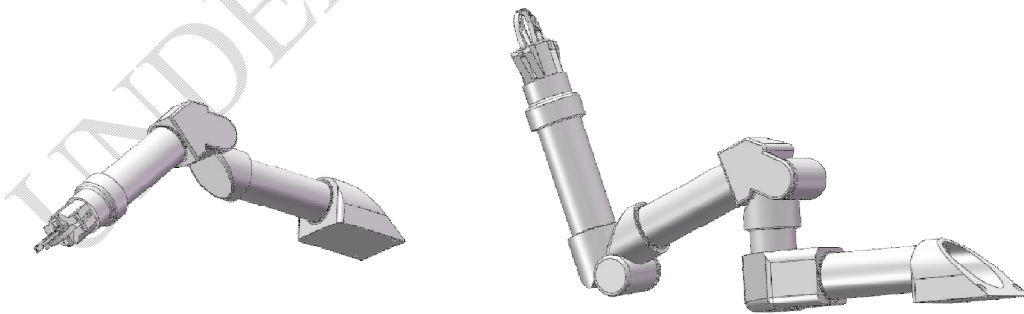


Figure 6 Underwater camera device

1.6 Manipulator

Electric manipulators are more suitable for observation-class ROVs compared to hydraulic manipulators. One each of the three-function manipulator ALPHA3 and the five-function manipulator ALPHA5 are selected. The manipulator arm of this manipulator is made of high-strength plastic, which can effectively reduce the initial weight of the ROV and is especially suitable for observation-class ROVs. It only weighs 1.3kg in air, has a maximum working radius of up to 400mm, and a maximum lifting force of up to 2kg. The two manipulators are installed at the front of the ROV for collaborative use. To adapt to different usage environments, a four-claw gripper, standard clamp, parallel clamp, and wire cutter can be replaced at the end of the manipulator.

The two types of underwater manipulators of this model have embedded controllers installed internally, requiring no additional POD data structure for control, with the control



protocol being the RS232/RS485 communication protocol. The control is simple and efficient.

Figure 7 Manipulator

2 Hydrodynamic Calculation

The study focuses on an observation-class ROV underwater robot with a body length $L=700\text{mm}$, width $W=420\text{mm}$, height $H=300\text{mm}$, weight of 26.8kg , displacement of 0.0259m^3 , and buoyancy slightly greater than gravity.

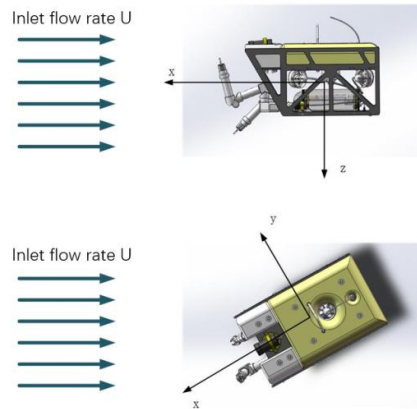


Figure 8 Schematic diagram of flow velocity at the entrance of the solution domain

$$\begin{cases} u = U \cos \beta \\ v = -U \sin \beta \end{cases} \quad \#(1)$$

2.1 Model Building and Grid Division

The dimensions of the simulated pool are $20\text{m} \times 20\text{m} \times 40\text{m}$, satisfying in steady-state simulation that the upstream distance of the ROV's front is greater than 1.5 times the length of the ROV body, and the wake is greater than 3 times the length of the ROV body. The simulated speed range is set to the ROV's common speed, i.e., $0 \sim 1\text{m/s}$. The simulation interval speed is 0.1m/s . When simulating skew motion, the inlet flow U is set to 1m/s , the bow angle β simulation range is -10° to 10° , and the interval angle is 2° .

To accurately calculate results and improve computational efficiency, during the hydrodynamic calculation of the ROV using Fluent software, a sub-domain must be divided in the above simulated pool, and the model must be appropriately simplified. The dimensions are set to $7\text{m} \times 7\text{m} \times 12\text{m}$. During calculation, the external flow domain grid size is set to 4mm , the sub-domain grid size is set to 1mm , and the model face grid is set to 0.1mm . The total number of grids in the entire domain is more than 2.32 million, and the average grid quality is 0.85. The turbulence $SSTk - \omega$ model is selected.

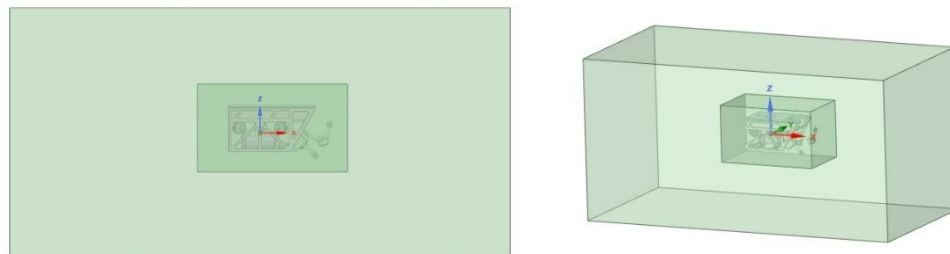


Figure 9 Solve the domain model

Figure 10 Outer basin grid division

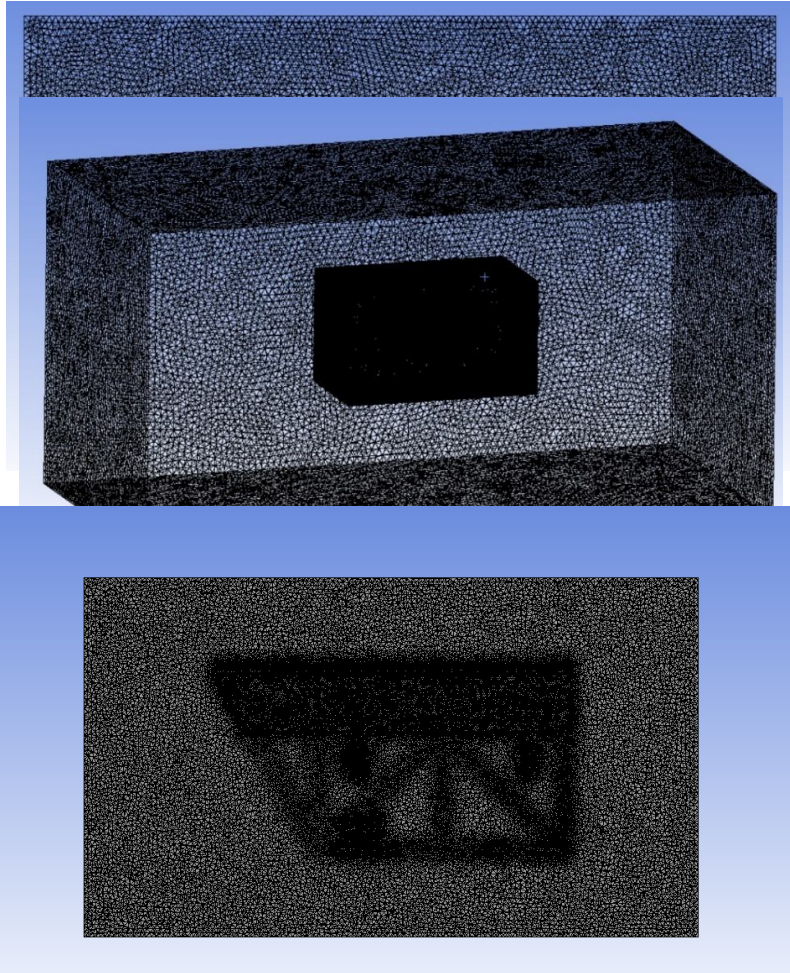


Figure 11 Subwatershed meshing

Figure 12 Mesh X-Z profiles

2.2 Steady-State Motion Analysis

During steady-state longitudinal, lateral, and upward motion simulations, the entrance flow speed of the solution domain is set from 0.1m/s to 1m/s for simulation simulation every 0.1m/s, with the ROV moving only in the x 、 y 、 z axial direction. During the ROV skew steady-state analysis, the entrance flow speed of the solution domain is set to 1m/s, and the skew angle range is -10° to 10° , with an interval of 2° . Figures 13 to 15 show the force conditions of the ROV at different speeds in the x 、 y 、 z axial direction, and Figure 16 shows the force condition in the z axial direction when the speed in the x 、 y axial direction

is 1m/s and the bow angle range is -10° to 10° .

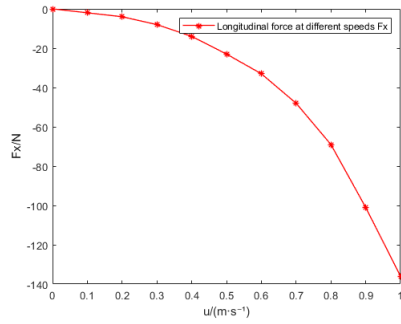


Figure 13 Fx in longitudinal motion

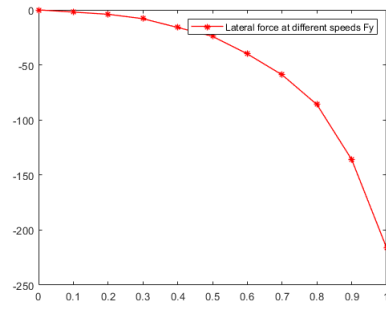


Figure 14 Fy during lateral movement

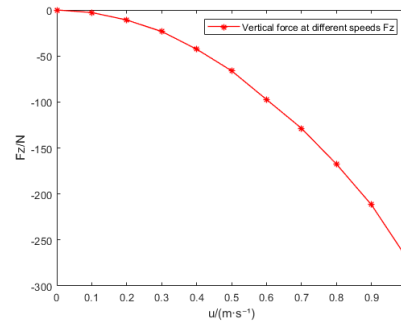


Figure 15 Fz in vertical motion

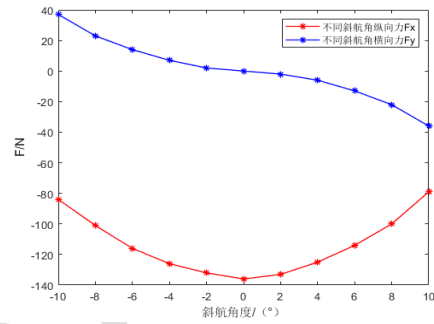


Figure 16 Fx and Fy at yaw

When the entrance flow speed is 1m/s, the velocity flow field cloud maps in each direction are as shown in the figure:

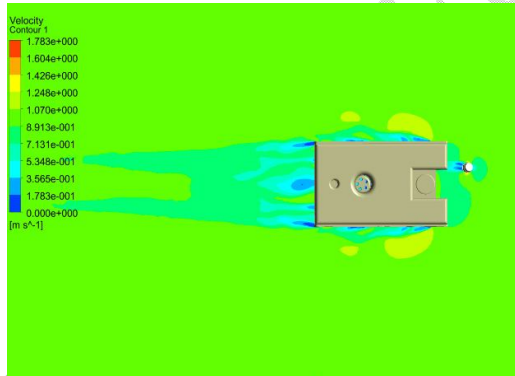


Figure 17 Longitudinal movement

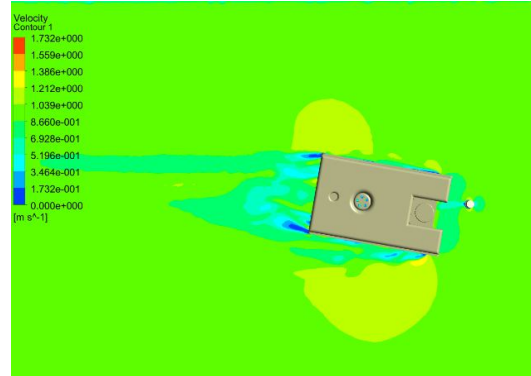


Figure 18 10° oblique motion

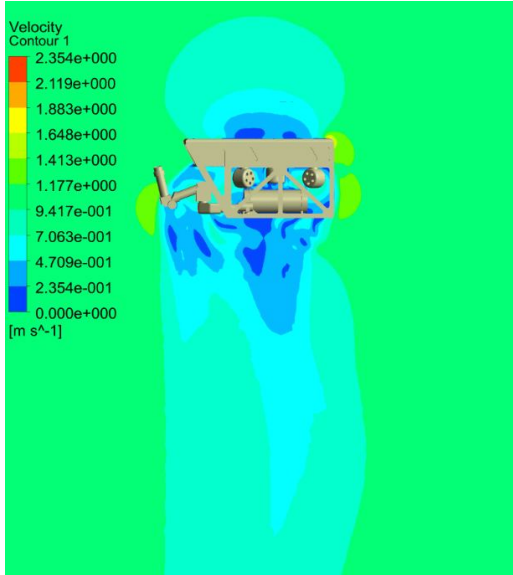


Figure 19 Vertical movement

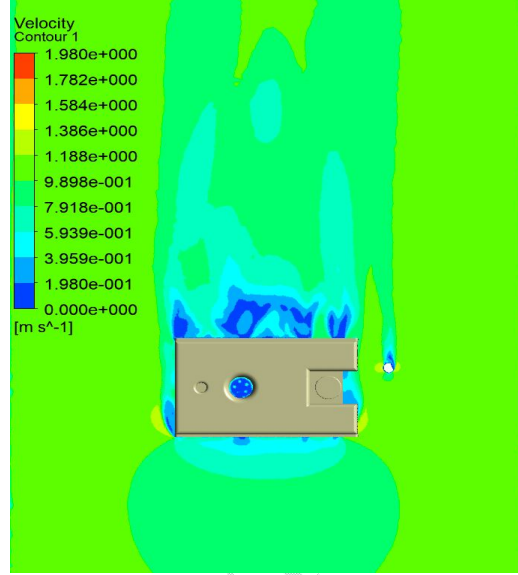


Figure 20 Lateral movement

Through the above Fluent steady-state motion simulation of the force results of the ROV under different working conditions, and coupled with the viscous hydrodynamic expression (2) during steady-state motion, the first-order viscous hydrodynamic coefficient $^{[6]}X_u$ 、 Y_v 、 Z_w 、 N_r and the second-order viscous hydrodynamic coefficient in the dynamic equation can be obtained^[9]、 $Y_{v|v}$ 、 $Z_{w|w}$ 、 $N_{r|r}$ 、

$$\begin{aligned}
 X &= X_u u + X_{uu} u^2 + X_{u|u} |u| |u| + X_{vv} v^2 + X_{rr} r^2 \\
 &\quad + X_{vr} vr + X_{ww} w^2 + X_{qq} q^2 + X_{wq} wq \\
 Y &= Y_v + Y_{ur} uv + Y_{ur} ur + Y_{v|v} |v| |v| + Y_{r|r} |r| |r| + Y_{v|r} |v| |r| \quad \#(2) \\
 Z &= Z_w + Z_{uw} uw + Z_{uq} uq + Z_{ww} |w| |w| + Z_{q|q} |q| |q| + Z_{wq} |w| |q| \\
 N &= N_r + N_{uv} uv + N_{ur} ur + N_{v|v} |v| |v| + N_{r|r} |r| |r| + N_{v|r} |v| |r|
 \end{aligned}$$

The inertial hydrodynamic coefficients $X_{\dot{u}}$ 、 $Y_{\dot{v}}$ 、 $Z_{\dot{w}}$ 、 $N_{\dot{r}}$ needed in the calculation are obtained through empirical formulas. Thus, all the hydrodynamic coefficients required in the simplified dynamic model of the ROV have been obtained, as shown in Table 1:

Table 1 Hydrodynamic coefficient calculation

X_u	-14.289
Y_v	-98.59
Z_w	-143.236
N_r	-65.273
$X_{\dot{u}}$	-72.489
$Y_{\dot{v}}$	-84.632
$Z_{\dot{w}}$	-146.581
$N_{\dot{r}}$	-26.942
$X_{u u }$	-153.685
$Y_{v v }$	-36.286
$Z_{w w }$	49.154
$N_{r r }$	-19.261

Conclusion

This paper introduces the structural problems in the ROV design process, analyzes the material and working environment of the main components of the ROV; and models and selects sensors and actuators for the control part based on the working needs of the ROV. This paper also provides a method to perform steady-state analysis on the model under different conditions using Fluent, and obtain the hydrodynamic coefficients by fitting the analysis results with formulas. The hydrodynamic coefficients can characterize the underwater motion characteristics of different underwater robots. Correct and efficient calculation of hydrodynamic coefficients is of great significance to the study of the motion laws of underwater robots.

References

- [1] Chen Deyun. Automatic Deep Sea Exploration Machine [J]. Navigation, 1989, 3: 43.
- [2] Mao Jiuyu. "Haitrench" Submerges to the Bottom of Ten Thousand Meters Sea [J]. Robot Technology and Application, 1996, (02): 24-5.
- [3] Liang Bo, Zhao Hongyu, Wang Nan. Early Development of Underwater Robots in China [J]. Science, 2022, 74(03): 53-6+69.
- [4] Successful Sea Trial of "Hailong" Unmanned Tethered Submersible [J]. Marine World, 2010, (12): 5.
- [5] Ping Wei, Ma Xiafei, Zhang Jinhua, et al. "Haima" Unmanned Remote Control Submersible [J]. Ship Science and Technology, 2017, 39(15): 138-41.
- [6] Yan Yinpo, Yu Fujie, Chen Yuan. Calculation of Hydrodynamic Coefficients and Dynamic Modeling of Open-frame Underwater Robots [J]. Acta Armamentarii, 2021, 42(09): 1972-86.
- [7] Peng Bo, Tian Junwei, Sun Jianglong, et al. Structural Design and Research of Observation-class ROV [J]. Manufacturing Automation, 2018, 40(12): 118-20.
- [8] Pei Lei, Tian Junwei, Su Yu, et al. Structural Design and Mechanical Simulation of Ultra-small Modular ROV's Sealed Cabin [J]. Machine Tool & Hydraulics, 2018, 46(21): 54-9.
- [9] Qiu Lei. Calculation of Ship Maneuvering Related Viscous Flow and Hydrodynamics [D]; Wuhan University of Technology, 2003.